

Received November 27, 2020, accepted December 10, 2020, date of publication December 23, 2020, date of current version February 10, 2021.

Digital Object Identifier 10.1109/ACCESS.2020.3046671

# Power Flow Calculation of Distribution Network With Multiple Energy Routers

LANG HUANG<sup>1</sup>, (Student Member, IEEE), CHENXI ZONG<sup>2</sup>, XU YANG<sup>1</sup>, (Member, IEEE), WENJIE CHEN<sup>1</sup>, (Member, IEEE), YIXIN ZHU<sup>2</sup>, (Member, IEEE), AND KAITAO BI<sup>2</sup>, (Member, IEEE)

<sup>1</sup>College of Electrical Engineering, Xi'an Jiaotong University, Xi'an 710049, China

<sup>2</sup>College of Internet of Things Engineering, Jiangnan University, Wuxi 214122, China

Corresponding author: Chenxi Zong (zongchenxi234@163.com)

This work was supported in part by the National Natural Science Foundation of China (NSFC) under Grant 51807079.

**ABSTRACT** Energy router is an emerging device based on power electronic technology, which can realize the flexible distribution of electric energy in the power system. Therefore, the use of energy routers to improve the operating conditions of the power system not only has broad development prospects, but also brings economic benefits. In this regard, this paper proposes a steady-state model of a single energy router and considers the loss of the DC/DC transformer, establishes a power flow equation with multiple energy routers, and proposes a distribution network power flow alternate iteration that takes into account multiple energy routers Calculation method. A case study of an improved IEEE-33 system with multiple energy routers under different working conditions is carried out. The calculation results show that the alternate iterative power flow calculation method used in this paper is effective and feasible, and it reasonably reflects that the network analysis model with multiple energy routers can achieve stable operation, and it can improve the node voltage and reduce the active power loss of the grid. It makes the operation of the distribution network more flexible.

**INDEX TERMS** Multiple energy routers, distribution network, DC/DC transformer, alternate iterative, power flow calculation.

## I. INTRODUCTION

Energy is one of the foundations for the survival and development of human society, and the problem of energy shortage is also a key issue that people have paid attention to in recent years. The energy development model based on fossil energy consumption not only has limitations in the total amount, but also causes certain pollution to the environment [1], [2]. In order to solve the problem of energy shortage and environmental protection, countries all over the world will focus on the active research on the development and application of renewable energy [3].

In the traditional power system, power regulation mainly relies on the generator set, which is mostly controlled in a centralized manner by means of electric energy coordination. In addition, the transformer, as a key link in the system,

The associate editor coordinating the review of this manuscript and approving it for publication was Bin Zhou.

only has the function of voltage conversion but not power adjustment and distribution, which means that a new type of power transformation equipment is urgently needed to meet the needs of energy Internet construction [4]. For this reason, the FREEDM Center of North Carolina State University in the United States proposed the concept of energy routers. This design concept is derived from information routers and switches in the Internet. The energy flow is regarded as the information flow, and the free distribution and transmission of electric energy are realized through the energy router in the grid [6], [7].

At present, the research on energy routers mainly focuses on its structural design [8], [9], transient simulation [10], [11] and optimized control strategy [12]–[14]. In reference [8], the design method of key parameters of energy router is proposed based on the principle of energy balance, and the design of high-frequency transformer inductance, leakage inductance and bus capacitance is analyzed. Based on

reference [8], a design method of the main circuit of modular multi-interface energy router is proposed in reference [9]. The design methods of energy storage, converter, common DC bus and energy interface are emphatically discussed. Reference [12] established an energy router model based on AC/DC hybrid network based on the traditional AC micro-grid energy router model, and analyzed the relationship and limitation of the rectifier stage phasor under different working modes in the case of cascade connection. The simulation shows that the energy router can effectively improve the availability of the microgrid. Reference [11] uses the idea of decentralized and autonomous coordination control to simulate and analyze multi-port energy routers, and realizes the decentralized and autonomous coordination capabilities of energy routers, and improves the reliability and efficiency of transmission. Reference [12] adds a self-storage control strategy to the control of the energy router, which can stabilize the voltage of the energy subnet even when the input power is short of power, and provide short-term energy supply when the network is switched. Reference [13] proposed an energy router model based on AC/DC hybrid microgrid, which can be used for multiple voltage levels. Then, the idea of power coordinated control is used to ensure the stable operation of the AC/DC hybrid network with energy router while meeting the required power for the output part of the grid connected. In [14], an energy layered coordinated control strategy and seamless handover method for energy router are proposed to make the system run more stable.

At present, the research on energy router design, simulation and optimization has gradually matured, but there are still few researches on the establishment of energy router steady-state models and the role played in network operation [15]. The research on the steady-state model of energy routers is mostly limited to the research on the steady-state model of a single energy router, and most of them do not consider the loss calculation models of energy routers. With the continuous development of the power system, the distribution network with a single energy router can no longer meet the needs of the development of the distribution network, and the cooperation and operation of multiple energy routers is the inevitable trend of the future development of the distribution network. Therefore, it is necessary to discuss in depth the power flow calculation method of the distribution network with multiple energy routers to lay the foundation for the flexible operation and optimized control of the power grid with multiple energy routers.

The basic solution methods for power flow calculation of distribution networks with energy routers can be divided into two types: unified solution method and alternating iteration method. The alternating iterative method divides the power flow calculation module into a distribution network module and an energy router module, which are solved separately. Compared with the unified solution method, the alternating iteration method does not need to augment the Jacobian matrix of the distribution network. When calculating the

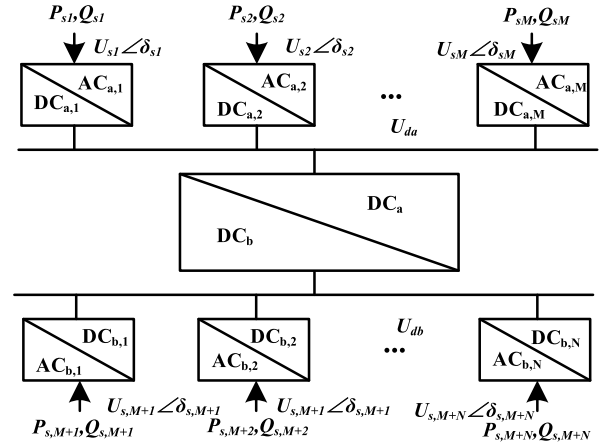


FIGURE 1. Structure diagram of energy router.

power flow of the energy router module, there is no need to modify the Jacobian matrix of the AC distribution network. Therefore, compared with the unified solution method, the alternating iteration method is easier to implement, less computationally expensive, and more efficient.

In this regard, this paper proposes a general analysis method for power flow calculation of multi-energy router distribution network considering the losses of energy routers. Firstly, the basic steady-state calculation model of a single energy router is established, and the loss model of energy router is taken into account; Secondly, based on the steady-state calculation model of a single energy router, the power flow equation with multiple energy routers is derived; Then, an alternating iteration method is proposed to solve the power flow problem with multiple energy routers; Finally, a case study of the improved IEEE-33 system is carried out to verify the effectiveness of the proposed model.

## II. STEADY STATE MODEL OF ENERGY ROUTER

Energy router is a kind of power equipment that integrates information technology and power electronic conversion technology to realize the efficient utilization and transmission of distributed energy. Energy routers are an indispensable part of the realization of energy Internet. A single energy router can no longer meet the needs of the development of the distribution network [16], and the cooperative operation of multiple energy routers has become an inevitable trend of development. Features of multiple energy routers are: 1) Each energy router can provide a standardized plug-and-play interface to complete the safe startup and mode determination of the equipment; 2) Have the ability to detect and isolate faults and formulate energy management plans; 3) Multiple energy routers adopt solid-state transformer type (SST) structure, which can reduce the reactive power loss of the power system by independently setting the bus voltage of each port; 4) It can realize the active control of power flow direction and size, and at the same time complete the optimization of power quality.

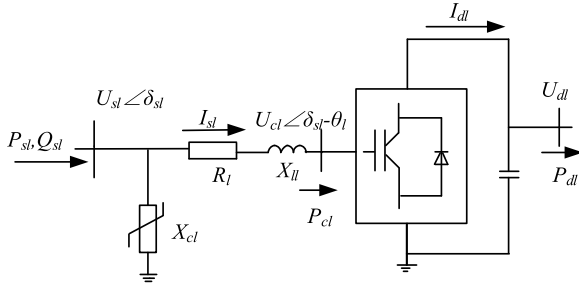


FIGURE 2. Energy router AC/DC converter model.

### A. AC/DC CONVERTER MODEL

The equivalent circuit of AC/DC converter is shown as in Fig. 2 [17]. The AC/DC converter model is composed of reactor, bridge, AC filter and DC capacitor.  $R_l$  is the loss of  $l$ -port converter,  $U_{cl}$  is the fundamental voltage of  $l$ -port converter.  $X_l$  and  $X_{cl}$  are the fundamental reactance of  $l$ -port converter and AC filter respectively. Let  $P_{sl}$  and  $Q_{sl}$  denote the active power and reactive power injected into port  $l$  from the side of the grid, respectively, the amplitude of the AC grid side voltage is denoted as  $U_{si}$ , the corresponding angle is denoted as  $\delta_{sl}$ , and the phase angle difference between  $U_{cl}$  and  $U_{si}$  is  $\theta_l$ . According to different control objectives, the energy router can control the power grid containing the energy router by independently adjusting  $P_{sl}$  and  $Q_{sl}$ .

For the convenience of description, the conductance and susceptance of AC/DC converter are expressed as

$$\begin{cases} G_l = R_l / (R_l^2 + X_l^2) \\ B_l = X_l / (R_l^2 + X_l^2) \\ G_{cl} = 1 / X_{cl} \end{cases} \quad (1)$$

On this basis, according to Kirchhoff's law, the  $P_s$  and  $Q_s$  injected into port  $l$  of the energy router can be expressed as:

$$\begin{cases} P_{sl} = G_l (U_{sl}^2 - U_{sl} U_{cl} \cos \theta_l) + B_l U_{sl} U_{cl} \sin \theta_l \\ Q_{sl} = B_l (U_{sl}^2 - U_{sl} U_{cl} \cos \theta_l) - G_l U_{sl} U_{cl} \sin \theta_l + B_{cl} U_{sl}^2 \end{cases} \quad (2)$$

where  $U_{si}$ ,  $G_l$  and  $B_l$  are generally fixed values in the system, it is not difficult to find that the size and flow direction of  $P_{sl}$  and  $Q_{sl}$  can be controlled by changing  $\theta_l$  and  $U_{cl}$ .

According to the energy conservation theorem, the expression of active power  $P_{dl}$  at DC side is as follows:

$$P_{dl} = U_{dl} I_{dl} = G_l (-U_{cl}^2 + U_{sl} U_{cl} \cos \theta_l) + B_l U_{sl} U_{cl} \sin \theta_l \quad (3)$$

where  $I_{dl}$  is the current flowing through the DC side,  $U_{dl}$  is the voltage at the DC side, and the active power  $P_{dl}$  at the DC side is the product of the two.

The relationship between  $U_{cl}$  and DC side voltage  $U_{dl}$  can be expressed as follows:

$$U_{cl} = k_l U_{dl} \quad (4)$$

where  $k_l$  represents the control coefficient of the voltage, and the modulation strategy of the converter and the wiring form of the line determine its value.

$$k_l = \mu M / \sqrt{2} \quad (5)$$

where  $\mu$  represents the utilization ratio of DC voltage. When sine pulse width modulation is used, its value is  $\sqrt{3}/2$ , and when space vector modulation is used, its value is 1.  $M$  represents the modulation coefficient, and its modulation range is  $0 \leq M \leq 1$ . Therefore, When the AC/DC converter adopts space vector modulation, the value range of  $k_l$  is  $0 \leq k_l \leq 1/\sqrt{2}$ .

### B. DC/DC CONVERTER MODEL

The voltage value on each side of the DC/DC converter can be realized by controlling the power electronics. Based on the principle of internal power conservation, the power loss balance constraints of primary and secondary sides in energy router can be expressed as follows:

$$U_{da} I_{da} + U_{db} I_{db} - (P_{sta} + P_{dyn}) = 0 \quad (6)$$

where  $I_{da}$  and  $I_{db}$  are the sum of the primary and secondary currents;  $P_{sta}$  is the static power loss of the DC/DC converter;  $P_{dyn}$  is the dynamic power loss of the DC/DC converter.  $I_{da}$  and  $I_{db}$  can be further expanded into

$$\begin{cases} I_{da} = \sum_{i=1}^M I_{di} \\ I_{db} = \sum_{j=M+1}^{M+N} I_{dj} \end{cases} \quad (7)$$

(1)  $I_{di}$  and  $I_{dj}$  can be expressed as follows:

$$\begin{cases} I_{di} = -G_i (k_i^2 U_{d\phi} - k_i U_{si} \cos \theta_i) + B_i k_i U_{si} \sin \theta_i \\ I_{dj} = -G_j (k_j^2 U_{d\psi} - k_j U_{sj} \cos \theta_j) + B_j k_j U_{sj} \sin \theta_j \end{cases} \quad (8)$$

(2) The static power loss  $P_{sta}$  of DC/DC converter is mainly produced by isolated transformer. Its skeleton structure, core material and switching frequency are important factors affecting the static power loss  $P_{sta}$ . according to Steinmetz equation, the static power loss characteristics of the transformer in the converter can be expressed as:

$$P_{sta} = FKf^\alpha B^\beta \quad (9)$$

where  $K$ ,  $f^\alpha$  and  $B^\beta$  are constants when the core material, structure and switching frequency are selected;  $F$  is the flux waveform coefficient.

(3)  $P_{dyn}$  is determined by the power provided by both sides of DC/DC transformer, and can be estimated by the following equation [18]:

$$\begin{aligned} P_{dyn} = & I_{d\phi}^2 R_{d\phi} + \left( \frac{I_{d\phi} f \phi}{I_{d\phi} 0 f \phi 0} \right)^2 P_{we\phi 0} \\ & + \left( \frac{I_{d\phi}}{I_{d\phi} 0} \right)^2 \left( \frac{f \phi}{f \phi 0} \right)^{0.8} P_{se\phi 0} \\ & + I_{d\psi}^2 R_{d\psi} + \left( \frac{I_{d\psi} f \psi}{I_{d\psi} 0 f \psi 0} \right)^2 P_{we\psi 0} \end{aligned}$$

$$+ \left( \frac{I_{d\psi}}{I_{d\psi 0}} \right)^2 \left( \frac{f_{\psi}}{f_{\psi 0}} \right)^{0.8} P_{se\psi 0} \quad (10)$$

where  $f$  is the working PWM frequency of the DC/DC transformer and  $I$  is the DC current on both sides of the DC/DC transformer. When the DC/DC transformer operates under  $I_{d0}$  and  $f_0$  conditions,  $P_{we0}$  is the basic eddy current loss in the winding and  $P_{se0}$  is the basic stray loss in metal structure parts. Once the PWM frequency is fixed, the dynamic power consumption can be expressed as follows:

$$P_{dyn} = I_{d\phi}^2 R_{E\phi} + I_{d\psi}^2 R_{E\psi} \quad (11)$$

For the energy router, it is necessary to relax the active power control of one port to meet the power loss balance constraint of the energy router. In this paper, the  $M$  port on the secondary side of each energy router is set as the relaxed port.

### C. STEADY STATE POWER FLOW MODEL OF MULTIP-LE ENERGY ROUTERS

When the number of energy routers in the system is  $n$ , they can be labelled and represented by the set  $S$ :

$$S = \{ER_1, \dots, ER_t, \dots, ER_n\}, t = 1, 2, \dots, n \quad (12)$$

This article assumes that the port of the energy router adopts the PQ control strategy, and the voltage control coefficient and phase angle difference of the energy router in the power flow analysis are unknown. Assuming that the  $ER_t$  contains  $M_t$  primary side port,  $N_t$  secondary side port, the  $l$ th port and AC grid exchange of reactive power, reactive power can be expressed as  $P_{sl}^t, Q_{sl}^t$ , at this time the energy router port  $l$  node power equation is:

$$\begin{cases} \Delta P_{sl}^t = P_{sl}^t - (G_l^t (U_{sl}^t U_{sl}^t - U_{sl}^t U_{cl}^t \cos \theta_l^t) + B_l^t U_{sl}^t U_{cl}^t \sin \theta_l^t) \\ \Delta Q_{sl}^t = Q_{sl}^t - B_l^t (U_{sl}^t U_{sl}^t - U_{sl}^t U_{cl}^t \cos \theta_l^t) + G_l^t U_{sl}^t U_{cl}^t \sin \theta_l^t \\ -B_{cl}^t U_{sl}^t U_{sl}^t \end{cases} \quad (13)$$

where  $U_{sl}^t$  is the AC voltage value connected to the  $l$ th port of  $ER_t$  and the external power grid,  $U_{cl}^t$  is the voltage value of the AC node inside the  $l$ th port of  $ER_t$ , and the phase angle difference between the two is expressed as  $\theta_l^t$ ;  $\Delta P_{sl}^t$  and  $\Delta Q_{sl}^t$  are the deviation of active power and reactive power of  $ER_t$ .

The power loss balance of  $ER_t$  is:

$$\Delta P_l^t = U_{da} I_{da} + U_{db} I_{db} - (P_{sta} + P_{dyn}) \quad (14)$$

Combining equation (3) and equation (7), we can get equation (15):

$$\begin{aligned} \Delta P_l^t &= U_{da} \sum_{l=1}^{M_t} (-G_l^t (k_l^t k_l^t U_{da} - k_l^t U_{sl}^t \cos \theta_l^t) + B_l^t k_l^t U_{sl}^t \sin \theta_l^t) \\ &+ U_{db} \sum_{l=M_t+1}^{M_t+N_t} (-G_l^t (k_l^t k_l^t U_{db} - k_l^t U_{sl}^t \cos \theta_l^t) \\ &+ B_l^t k_l^t U_{sl}^t \sin \theta_l^t) \end{aligned}$$

$$\begin{aligned} &- \left( \sum_{l=1}^{M_t} (-G_l^t (k_l^t k_l^t U_{da} - k_l^t U_{sl}^t \cos \theta_l^t) + B_l^t k_l^t U_{sl}^t \sin \theta_l^t) \right)^2 \\ &\times R_{E\phi} \\ &- \left( \sum_{l=M_t+1}^{M_t+N_t} (-G_l^t (k_l^t k_l^t U_{db} - k_l^t U_{sl}^t \cos \theta_l^t) \right. \\ &\left. + B_l^t k_l^t U_{sl}^t \sin \theta_l^t) \right)^2 R_{E\psi} \\ &- P_{sta} \end{aligned} \quad (15)$$

Equations (13) and (15) constitute the power flow equation of  $ER_t$ . In addition to the relaxed port, the  $P_{sl}^t$  and  $Q_{sl}^t$  of each port can be set as the control target, and the  $Q_{sl}^t$  of the relaxed port can also be determined. In this case,  $ER_t$  has  $M_t+N_t-1$  active power and  $M_t+N_t$  reactive power is known. With a balance constraint of power loss, there are  $2^*(M_t+N_t)$  equations that are known. Then there are  $2^*(M_t+N_t)$  equations that are unknown, which are  $M_t+N_t$  phase angle difference  $\theta_l^t$  and  $M_t+N_t$  voltage control coefficient  $k_l^t$ . For example, the active power calculation of the balance node of the power system, after all  $\theta_l^t$  and  $k_l^t$  are obtained, the active power  $P_{s,M+N}^t$  of the relaxation port can be determined.

The power flow equation of  $ER_t$  can be solved by the Newton-Raphson method, and the iterative equation is (16), as shown at the bottom of the next page: where  $\Delta F^t$  is the deviation value of the  $ER_t$  power flow equations,  $\Delta X^t$  is the variable of the  $ER_t$  power flow equations, and  $J^t$  is the Jacobian matrix of the  $ER_t$  power flow equations.

The Jacobian matrix  $J^t$  can be expressed as:

$$J = \begin{pmatrix} \frac{\partial(\Delta P_s^t)}{\partial k^t} & \frac{\partial(\Delta P_s^t)}{\partial \theta^t} \\ \frac{\partial(\Delta Q_s^t)}{\partial k^t} & \frac{\partial(\Delta Q_s^t)}{\partial \theta^t} \\ \frac{\partial(\Delta P_L^t)}{\partial k^t} & \frac{\partial(\Delta P_L^t)}{\partial \theta^t} \end{pmatrix} \quad (17)$$

Each matrix block in the equation represents the partial derivative of the deviation value of the power flow equation system to the variable. The specific expression is as follows:

$$\begin{cases} \partial(\Delta P_s^t)/\partial k^t = G^t U_d U_s \cos \theta^t - B^t U_d U_s \sin \theta^t \\ \partial(\Delta P_s^t)/\partial \theta^t = -G^t k^t U_d U_s \sin \theta^t - B^t k^t U_d U_s \cos \theta^t \\ \partial(\Delta Q_s^t)/\partial k^t = B^t U_d U_s \cos \theta^t + G^t U_d U_s \sin \theta^t \\ \partial(\Delta Q_s^t)/\partial \theta^t = -B^t k^t U_d U_s \sin \theta^t + G^t k^t U_d U_s \cos \theta^t \\ \partial(\Delta P_L^t)/\partial k^t = U_d (-G^t (2k^t U_d - U_s \cos \theta^t) + B^t U_s \sin \theta^t) \\ -2R_E (-G^t (2k^t U_d - U_s \cos \theta^t) + B^t U_s \sin \theta^t) \\ (-G^t (k^t k^t U_d - k^t U_s \cos \theta^t) + B^t k^t U_s \sin \theta^t) \\ \partial(\Delta P_L^t)/\partial \theta^t = U_d (-G^t k^t U_s \sin \theta^t + B^t k^t U_s \cos \theta^t) \\ -2R_E (-G^t k^t U_s \sin \theta^t + B^t k^t U_s \cos \theta^t) \\ (-G^t (k^t k^t U_d - k^t U_s \cos \theta^t) + B^t k^t U_s \sin \theta^t) \end{cases} \quad (18)$$

According to the initial conditions given by the system, the combined equations (16)-(18) can perform power flow calculation and analysis on  $ER_t$ .

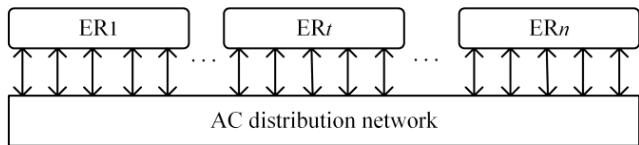


FIGURE 3. Network diagram with multiple energy routers.

### III. POWER FLOW CALCULATION METHOD FOR MULTIPLE ENERGY ROUTERS

#### A. POWER GRID MODEL OF MULTIPLE ENERGY ROUTERS

A schematic diagram of an AC power grid with multiple energy routers is shown in Figure 3. There are  $n$  multi-port energy routers for energy exchange with the AC power grid.

The model of the AC distribution network is a nodal power equation reflecting the relationship between nodal power, nodal voltage and phase angle:

$$P_{grid,i} = V_i \sum_{j \in i} V_j (G_{ij} \cos(\theta_{ij}) + B_{ij} \sin(\theta_{ij})) \quad (19)$$

$$Q_{grid,i} = V_i \sum_{j \in i} V_j (G_{ij} \sin(\theta_{ij}) - B_{ij} \cos(\theta_{ij})) \quad (20)$$

In the equation,  $P_{grid,i}$  and  $Q_{grid,i}$  represent the reactive power and active power of AC distribution network at node  $i$ , respectively. The voltage of  $V_i$  and  $V_j$  at nodes  $i$  and  $j$ ,  $G_{ij}$  is the conductance of node admittance matrix,  $B_{ij}$  is the admittance of node admittance matrix, and  $\theta_{ij}$  is the phase angle difference between nodes  $i$  and  $j$ .

#### B. ALTERNATING ITERATION METHOD

The power flow of the AC distribution network power flow model with multiple energy routers can be solved by alternately solving the power flow equations between the AC grid and each energy router. The specific process is as follows:

1) The active power initialization of the balanced port: the initial active power injection of the slack port can be estimated according to the given value of the active power of other ports, as shown in equation (21).

$$P_{s,M_t+N_t}^t = - \sum_{l=1}^{M_t+N_t-1} P_{s,l}^t \quad (21)$$

For the internal parameters of the energy router, the initial values can be set as follows:

$$\theta_{l,0}^t = \arctan(P_{s,l}^t / (U_{sl}^t U_{sl}^t / X^t + U_{sl}^t U_{sl}^t / X_c^t - Q_{sl}^t)) \quad (22)$$

$$k_{l,0}^t = P_{s,l}^t X^t / U_{sl}^t U_d^t \sin \theta_{l,0}^t \quad (23)$$

2) AC system power flow calculation: According to the active power and reactive power values of the energy router

ports, the equivalent injected power of the AC distribution network nodes is updated. Assuming that the node  $h$  of the AC distribution network is connected to the port  $l$  of  $ER_t$ , the equivalent injected power of the node  $h$  of the AC distribution network is the sum of the original power of the AC system and the exchange power of the same port  $l$ . The equation can be expressed as:

$$\begin{cases} P_{grid,h} = P_{grid,h,0} + P_{sl}^t \\ Q_{grid,h} = Q_{grid,h,0} + Q_{sl}^t \end{cases} \quad (24)$$

After updating the equivalent injected power of the AC distribution network, the  $U_{sl}^t$  value of each node is updated accordingly, and the P-Q fast decomposition method is used to calculate the power flow of the AC distribution network.

3) Energy router port power flow calculation: Solve the variables  $\theta^t$  and  $k_l^t$  of  $ER_t$  by combining equations (16)-(18), update the active power  $P_{s,M+N}^{t,new}$  of the  $ER_t$  relaxation port, and calculate all energy router variables.

4) Convergence judgment: Calculate the changes in active power injected into the relaxation ports of all energy routers after this iteration. If it is small enough, terminate the iteration and give the result. Otherwise, turn to step 2).

$$\begin{aligned} & \max\{abs(P_{s,M_1+N_1}^{1,new} - P_{s,M_1+N_1}^1), \\ & \dots, abs(P_{s,M_t+N_t}^{t,new} - P_{s,M_t+N_t}^t) \\ & \dots, abs(P_{s,M_n+N_n}^{n,new} - P_{s,M_n+N_n}^n)\} < \varepsilon \end{aligned} \quad (25)$$

### IV. CASE STUDY

In this paper, an improved IEEE-33 node system with three energy routers is verified and analyzed [19]. The example topology is shown in Figure. 4. A two-port energy router is connected between nodes 12 and 30, a four-port energy router is connected between nodes 18, 22, 25 and 34, and a three-port energy router is connected between nodes 4, 26 and 19. Nodes 30, 34 and 19 are set as the relaxation ports of their energy router respectively, and the remaining nodes of energy router are controlled by PQ. The output of generators is extracted from the example files from Matpower version 6. The basic capacity of IEEE-33 node power distribution system is 10MVA. The rated voltage level of IEEE-33 distribution network is 12.66KV. The distribution network system consists of 33 nodes, 32 branches and 1 root node. The total load of distribution network is 5084.26+j2547.32KVA. The detailed parameters of the network can be referred to [20]. The capacity of the three energy routers is set to 0.5MVA. For the convenience of analysis and comparison, the original impedance values of AC / DC converter ports of all energy routers are the same. Each port impedance parameter

$$\begin{cases} \Delta F^t = J^t \Delta X^t \\ \Delta F^t = [\Delta P_{s,1}^t, \dots, \Delta P_{s,M_t+N_t-1}^t, \dots, \Delta Q_{s,1}^t, \dots, \Delta Q_{s,M_t+N_t}^t, \Delta P_L^t] \\ \Delta X^t = [k_1^t, \dots, k_{M_t+N_t}^t, \theta_1^t, \dots, \theta_{M_t+N_t}^t] \end{cases} \quad (16)$$

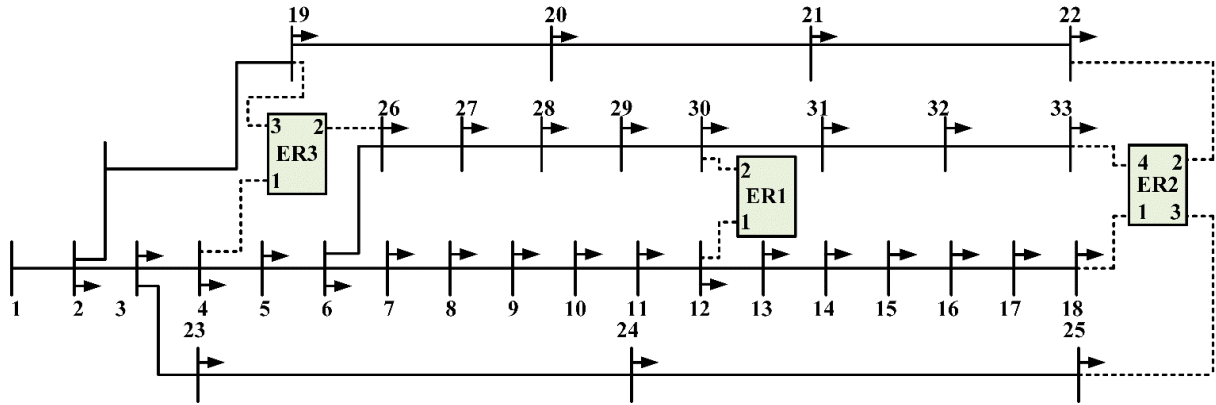


FIGURE 4. IEEE-33 node network topology with multiple energy routers.

$R$  is set to 0.002p.u.,  $X$  is set to 0.037p.u., and  $X_c$  is set to  $-18.2617$ p.u.. In this case, the convergence threshold  $\varepsilon$  is  $10^{-6}$ , and the unit values of the DC side voltage  $U_d$  are 1.5, 2 and 1.8 respectively.

**A. VERIFICATION OF POWER FLOW CALCULATION RESULTS**

According to the alternating iterative algorithm proposed in this paper, the power flow calculation of the AC distribution network with multiple energy routers is shown in Table 1. The system is iterated alternately, the running time is 22.49s, the number of iterations of the AC distribution network using the P-Q decomposition method is 12, and the number of iterations of the power flow of the energy router port is 15739. In the case, the initial values of  $P_{s,M1+N1}^1, P_{s,M2+N2}^2$  and  $P_{s,M3+N3}^3$  of the three energy routers balanced ports are  $-0.10$ MW,  $0$ MW and  $-0.03$ MW respectively, and the update times are 44. The network loss of the system is 0.178MW. At this time, the values of balanced ports  $P_{s,M1+N1}^{1\_new}, P_{s,M2+N2}^{2\_new}$  and  $P_{s,M3+N3}^{3\_new}$  remain unchanged at  $-0.098$ MW,  $-0.003$ MW and  $0.032$ MW, respectively. At the end of the alternate iteration process, the  $U_s, \theta$ , and  $k$  obtained from the power flow calculation are substituted into equations (12) and (14). The calculation results show that the values of  $\Delta P_{sl}^t, \Delta Q_{sl}^t$  and  $\Delta P_l^t$  are almost zero, which shows that the algorithm proposed in this paper is correct and effective. After adding multiple energy routers to calculate the power flow of distribution network, the minimum voltage of all nodes should be larger than the minimum value of original power flow voltage without energy router, and the maximum voltage per unit value of all nodes should be less than 1.05p.u..

**B. ANALYSIS OF DIFFERENT CASE RESULTS**

In order to verify the correctness of power flow calculation of distribution network under multiple energy routers and compare the impact of energy routers on the system under different conditions, three different cases are set up in this paper, and the results are shown in Table 2. Case 1 is to verify

TABLE 1. Calculation results of energy router.

ER	Port No	$P_s$ (MW)	$Q_s$ (MW)	$U_s$ (p.u.)	$k$	$\theta(^{\circ})$
1	1	0.100	-0.10	0.935	0.625	0.243
	2	-0.098	-0.10	0.930	0.622	-0.230
2	1	-0.100	-0.08	0.928	0.465	-0.237
	2	0.050	-0.07	0.992	0.496	0.107
	3	0.050	-0.06	0.970	0.485	0.111
	4	0.003	0.05	0.924	0.460	-0.008
3	1	0.050	-0.05	0.977	0.543	0.109
	2	-0.080	-0.05	0.953	0.530	-0.183
	3	0.032	0.05	0.997	0.552	0.055

TABLE 2. Calculation results in different cases.

Case No.	ER	Port No.	$P_s$ (MW)	$Q_s$ (MVar)	$U_s$ (p.u.)	$k$	$\theta(^{\circ})$
Case 1	1	1	-0.100	-0.10	0.946	0.632	-0.226
		2	0.102	-0.10	0.936	0.625	0.247
		1	-0.100	-0.10	0.939	0.471	-0.229
Case 2	2	2	0.100	-0.10	0.992	0.497	0.216
		3	0.100	-0.10	0.972	0.487	0.225
		4	-0.098	-0.10	0.933	0.467	-0.229
		1	-0.100	-0.10	0.980	0.545	-0.211
Case 3	3	2	-0.100	-0.10	0.958	0.534	-0.220
		3	0.202	-0.10	0.997	0.554	0.426
Case 1	1	1	-0.100	-0.10	0.926	0.619	-0.236
		2	0.102	-0.10	0.921	0.615	0.255
		1	0.100	0.08	0.905	0.450	0.239
Case 2	2	2	-0.050	0.07	0.991	0.493	-0.119
		3	-0.050	0.06	0.969	0.483	-0.123
		4	0.002	-0.05	0.916	0.458	0.005
		1	-0.050	0.05	0.975	0.540	-0.121
Case 3	3	2	0.080	0.05	0.946	0.523	0.175
		3	-0.028	-0.05	0.997	0.554	-0.060

the correctness of the power flow calculation results, and the results are given in Table 1. Case 2 is to further increase the voltage on the basis of case 1. Case 3 is to reverse the active power of case 1 (for example, port 3 of energy router 2 provides active power to the system in case 1, and the system provides active power to it in case 3). It should be pointed out that when the energy router is not considered, the system power loss is 0.203MW.

**TABLE 3.** Power flow calculation results of line in case 3.

Bus No.	From Node	To Node	$P_s$ (MW)	$Q_s$ (MVar)	$P_{loss}$ (MW)	$Q_{loss}$ (MVar)
1	1	2	3.93	2.45	0.012	0.01
2	2	3	3.54	2.2	0.054	0.03
3	3	4	2.5	1.62	0.021	0.01
4	4	5	2.41	1.48	0.02	0.01
5	5	6	2.33	1.44	0.041	0.04
6	6	7	1.1	0.51	0.002	0.01
7	7	8	0.9	0.4	0.005	0
8	8	9	0.69	0.3	0.004	0
9	9	10	0.63	0.28	0.004	0
10	10	11	0.56	0.26	0.001	0
11	11	12	0.52	0.23	0.001	0
12	12	13	0.56	0.29	0.004	0
13	13	14	0.49	0.25	0.001	0
14	14	15	0.37	0.17	0.001	0
15	15	16	0.31	0.16	0.001	0
16	16	17	0.25	0.14	0.001	0
17	17	18	0.19	0.12	0	0
18	2	19	0.28	0.18	0	0
19	19	20	0.22	0.19	0.001	0
20	20	21	0.13	0.15	0	0
21	21	22	0.04	0.11	0	0
22	3	23	0.89	0.52	0.003	0
23	23	24	0.8	0.46	0.005	0
24	24	25	0.37	0.26	0.001	0
25	6	26	1.13	0.87	0.003	0
26	26	27	0.99	0.8	0.003	0
27	27	28	0.93	0.77	0.011	0.01
28	28	29	0.86	0.74	0.007	0.01
29	29	30	0.73	0.66	0.004	0
30	30	31	0.42	0.16	0.001	0
31	31	32	0.27	0.09	0	0
32	32	33	0.06	-0.01	0	0

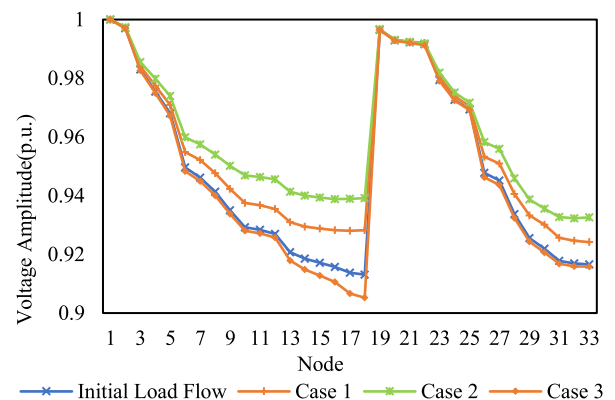
It can be seen from Table 1 and Table 2 that the energy router will play a certain role in raising the node voltage after participating in the network optimization control. After the IEEE-33 node distribution network introduces multiple energy routers, the network loss of the system when the energy router runs in Case 2 is only 0.137MW, which is 32.51% lower than before the energy router is added.

At the same time, it should be pointed out that the active power loss of the system increases to 0.212MW when the energy router is running in Case 3. It can be clearly seen that when the energy router is not well controlled, it will lead to a substantial increase in the active power loss of the system. Table 3 is the power flow calculation result of the line power and network loss in case 3, and Table 4 is the power flow calculation result of the power and network loss under the initial power flow. When the active power and reactive power of the energy router port are set improperly, as the active power and reactive power transmitted in the line increase, the line network loss further increases. It can be clearly seen that poor control of energy routers will worsen the power flow distribution of the system.

The node voltage of the system under different working conditions is shown in Figure.5. Compared with the initial power flow and case 1, it is not difficult to find that the coordinated optimal control of multiple energy routers can support the node voltage, especially the voltage of node 18 and node 33 has been improved., Furthermore in order to

**TABLE 4.** Calculation results of line power flow under initial power flow.

Bus No.	From Node	To Node	$P_s$ (MW)	$Q_s$ (MVar)	$P_{loss}$ (MW)	$Q_{loss}$ (MVar)
1	1	2	3.92	2.44	0.012	0.01
2	2	3	3.44	2.21	0.052	0.03
3	3	4	2.36	1.68	0.02	0.01
4	4	5	2.22	1.59	0.019	0.01
5	5	6	2.14	1.55	0.038	0.03
6	6	7	1.1	0.53	0.002	0.01
7	7	8	0.89	0.42	0.005	0
8	8	9	0.69	0.32	0.004	0
9	9	10	0.62	0.3	0.004	0
10	10	11	0.56	0.27	0.001	0
11	11	12	0.52	0.24	0.001	0
12	12	13	0.45	0.21	0.003	0
13	13	14	0.39	0.17	0.001	0
14	14	15	0.27	0.09	0	0
15	15	16	0.21	0.08	0	0
16	16	17	0.15	0.06	0	0
17	17	18	0.09	0.04	0	0
18	2	19	0.36	0.16	0	0
19	19	20	0.27	0.12	0.001	0
20	20	21	0.18	0.08	0	0
21	21	22	0.09	0.04	0	0
22	3	23	0.94	0.46	0.003	0
23	23	24	0.85	0.41	0.005	0
24	24	25	0.42	0.2	0.001	0
25	6	26	0.95	0.97	0.003	0
26	26	27	0.89	0.95	0.003	0
27	27	28	0.82	0.92	0.011	0.01
28	28	29	0.75	0.89	0.008	0.01
29	29	30	0.63	0.81	0.004	0
30	30	31	0.42	0.21	0.002	0
31	31	32	0.27	0.14	0	0
32	32	33	0.06	0.04	0	0

**FIGURE 5.** Node voltage under different conditions.

reduce power loss while not exceeding the maximum voltage of the original network, by controlling energy routers to work in Case 2, the system power loss can be significantly reduced. Energy routers help to optimize the system power flow distribution.

## V. CONCLUSION

In this paper, a steady-state power flow model of distribution network with multiple energy routers is established. Based on IEEE-33 system, the effect of operation state of distribution network with multiple energy routers is verified. The results show that the alternating iteration power

flow calculation method with multi energy router is correct and feasible. Through the coordinated operation of multiple energy routers, controlling the voltage of each port and the interactive power of distribution network can improve the minimum voltage of the system, reduce the active power loss of the system, and improve the operation state of the distribution network. Poor control measures cannot coordinate the operation of multiple energy routers, affecting the operation of the distribution network.

This paper discusses the power flow calculation method of distribution network with multiple energy routers, and how to realize the optimal operation of distribution network with multiple energy routers is the focus of the next work.

## REFERENCES

- [1] D. Xu, Q. Wu, B. Zhou, C. Li, L. Bai, and S. Huang, "Distributed multi-energy operation of coupled electricity, heating, and natural gas networks," *IEEE Trans. Sustain. Energy*, vol. 11, no. 4, pp. 2457–2469, Oct. 2020.
- [2] L. Xiong, X. Liu, C. Zhao, and F. Zhuo, "A fast and robust real-time detection algorithm of decaying DC transient and harmonic components in three-phase systems," *IEEE Trans. Power Electron.*, vol. 35, no. 4, pp. 3332–3336, Apr. 2020.
- [3] L. Xiong, X. Liu, D. Zhang, and Y. Liu, "Rapid power compensation based frequency response strategy for low inertia power systems," *IEEE J. Emerg. Sel. Topics Power Electron.*, early access, Oct. 19, 2020, doi: 10.1109/JESTPE.2020.3032063.
- [4] H. Wang, Y. Liu, B. Zhou, C. Li, G. Cao, N. Voropai, and E. Barakhtenko, "Taxonomy research of artificial intelligence for deterministic solar power forecasting," *Energy Convers. Manage.*, vol. 214, Jun. 2020, Art. no. 112909.
- [5] H. Guo, F. Wang, L. Zhang, and J. Luo, "A hierarchical optimization strategy of the energy router-based energy Internet," *IEEE Trans. Power Syst.*, vol. 34, no. 6, pp. 4177–4185, Nov. 2019.
- [6] L. Xiong, F. Zhuo, F. Wang, X. Liu, Y. Chen, M. Zhu, and H. Yi, "Static synchronous generator model: A new perspective to investigate dynamic characteristics and stability issues of grid-tied PWM inverter," *IEEE Trans. Power Electron.*, vol. 31, no. 9, pp. 6264–6280, Sep. 2016.
- [7] L. Xiong, F. Zhuo, X. Liu, Z. Xu, and Y. Zhu, "Fault-tolerant control of CPS-PWM-Based cascaded multilevel inverter with faulty units," *IEEE J. Emerg. Sel. Topics Power Electron.*, vol. 7, no. 4, pp. 2486–2497, Dec. 2019.
- [8] L. Xiong, F. Zhuo, F. Wang, X. Liu, and M. Zhu, "A fast orthogonal signal-generation algorithm characterized by noise immunity and high accuracy for single-phase grid," *IEEE Trans. Power Electron.*, vol. 31, no. 3, pp. 1847–1851, Mar. 2016.
- [9] B. Liu, W. Wu, C. Zhou, C. Mao, D. Wang, Q. Duan, and G. Sha, "An AC–DC hybrid multi-port energy router with coordinated control and energy management strategies," *IEEE Access*, vol. 7, pp. 109069–109082, 2019.
- [10] P. Yi, T. Zhu, B. Jiang, R. Jin, and B. Wang, "Deploying energy routers in an energy Internet based on electric vehicles," *IEEE Trans. Veh. Technol.*, vol. 65, no. 6, pp. 4714–4725, Jun. 2016, doi: 10.1109/TVT.2016.2549269.
- [11] Y. Chen, P. Wang, Y. Elasser, and M. Chen, "Multicell reconfigurable multi-input multi-output energy router architecture," *IEEE Trans. Power Electron.*, vol. 35, no. 12, pp. 13210–13224, Dec. 2020, doi: 10.1109/TPEL.2020.2996199.
- [12] Y. Liu, X. Chen, Y. Wu, K. Yang, J. Zhu, and B. Li, "Enabling the smart and flexible management of energy prosumers via the energy router with parallel operation mode," *IEEE Access*, vol. 8, pp. 35038–35047, 2020, doi: 10.1109/ACCESS.2020.2973857.
- [13] M. Chen, M. Xia, and Q. Chen, "Research on distributed source-load interaction strategy considering energy router-based active distribution network," *IEEE Access*, vol. 7, pp. 150505–150516, 2019, doi: 10.1109/ACCESS.2019.2946865.
- [14] P. Li, W. Sheng, Q. Duan, Z. Li, C. Zhu, and X. Zhang, "A Lyapunov optimization-based energy management strategy for energy hub with energy router," *IEEE Trans. Smart Grid*, vol. 11, no. 6, pp. 4860–4870, Nov. 2020.
- [15] J. Miao, N. Zhang, C. Kang, J. Wang, Y. Wang, and Q. Xia, "Steady-state power flow model of energy router embedded AC network and its application in optimizing power system operation," *IEEE Trans. Smart Grid*, vol. 9, no. 5, pp. 4828–4837, Sep. 2018.
- [16] X. Shi, Y. Xu, and H. Sun, "A biased min-consensus-based approach for optimal power transaction in Multi-Energy-Router systems," *IEEE Trans. Sustain. Energy*, vol. 11, no. 1, pp. 217–228, Jan. 2020.
- [17] T. Shu, X. Lin, S. Peng, X. Du, H. Chen, F. Li, J. Tang, and W. Li, "Probabilistic power flow analysis for hybrid HVAC and LCC-VSC HVDC system," *IEEE Access*, vol. 7, pp. 142038–142052, 2019, doi: 10.1109/ACCESS.2019.2942522.
- [18] J. Miao, N. Zhang, and C. Kang, "Generalized steady-state model for energy router with applications in power flow calculation," in *Proc. IEEE Power Electron. Soc. Gen. Meeting (PESGM)*, Jul. 2016, pp. 1–5, doi: 10.1109/PESGM.2016.7741416.
- [19] J. Miao, N. Zhang, and C. Kang, "Analysis on the influence of energy router on the optimal operation of distribution network," *Proc. Chin. Soc. Electr. Eng.*, vol. 37, no. 10, pp. 2832–2839, May 2017.
- [20] S. Jonnavithula and R. Billinton, "Minimum cost analysis of feeder routing in distribution system planning," *IEEE Trans. Power Del.*, vol. 11, no. 4, pp. 1935–1940, Oct. 1996.



**LANG HUANG** (Student Member, IEEE) received the B.S. degree in electrical engineering from Xi'an Jiaotong University, Xi'an, China, in 2011, where he is currently pursuing the Ph.D. degree. His research interests include model and control of multilevel converters, mainly focus on the topology and control of modular multilevel converter (MMC), control of power electronics transformer (PET), and model predictive control (MPC).



**CHENXI ZONG** received the B.S. degree from the Changzhou Institute of Technology, Changzhou, China, in 2019. She is currently pursuing the master's degree student in electrical engineering with the School of Internet of Things Engineering, Jiangnan University. Her research interests include energy router and power flow calculation of ac/dc hybrid systems.



**XU YANG** (Member, IEEE) received the B.S. and Ph.D. degrees in electrical engineering from Xi'an Jiaotong University, Xi'an, China, in 1994 and 1999, respectively. Since 1999, he has been a Member of the Faculty of the School of Electrical Engineering, Xi'an Jiaotong University, where he is currently a Professor. From November 2004 to November 2005, he was a Visiting Scholar with the Center of Power Electronics Systems (CPES), Virginia Polytechnic Institute and State University, Blacksburg, VA, USA. He then came back to Xi'an Jiaotong University, and engaged in the teaching and researches in power electronics and industrial automation area. His research interests include GaN based topologies, PWM control techniques, wireless power transmission systems, and packaging technologies.





**WENJIE CHEN** (Member, IEEE) received the B.S., M.S., and Ph.D. degrees in electrical engineering from Xi'an Jiaotong University, Xi'an, China, in 1996, 2002, and 2006, respectively. Since 2002, she has been a Member of the Faculty of the School of Electrical Engineering, Xi'an Jiaotong University, where she is currently a Professor. From January 2012 to January 2013, she was a Visiting Scholar with the Department of Electrical Engineering and Computer Science, University of Tennessee, Knoxville, TN, USA. She then came back to Xi'an Jiaotong University, and engaged in the teaching and researches in power electronics. Her main research interests include electromagnetic interference, active filters, and photovoltaic generation systems.



**KAITAO BI** (Member, IEEE) received the B.S. degree in electronic information engineering from the Harbin University of Science and Technology, Harbin, China, in 2012, and the M.S. degree and the Ph.D. degree in electrical engineering from the Harbin Institute of Technology, Harbin, in 2014 and 2019, respectively. He joined Jiangnan University, Wuxi, China, as an Associate Professor and a Master's Tutor, in 2019. His research interests include multilevel converters and high-power energy storage systems.

• • •



**YIXIN ZHU** (Member, IEEE) received the B.S., M.S., and Ph.D. degrees in electrical engineering from Xi'an Jiaotong University, Xi'an, China, in 2009, 2011, and 2015, respectively. He joined Jiangnan University, as a Lecturer, in 2016. He is currently with the School of IoT Engineering, Jiangnan University. His research interests include design, control and application of the high-power active power filter, photovoltaic grid-connected inverter, and modeling, analysis, and power management of the microgrid.